AFRL-SR-AR-TR-09-0184

REPORT DOCUMENTATION PAGE

1. REPORT DATE *(DD-MM-YYYY)*	2. REPORT TYPE	3. DATES COVERED *(From - To)*
31-03-2009	Final Performance Report	15-11-2005 – 30-11-2008

4. TITLE AND SUBTITLE

Chemical Modeling for Large-Eddy Simulation of Turbulent Combustion

5a. CONTRACT NUMBER

5b. GRANT NUMBER
FA9550-06-1-0060

5c. PROGRAM ELEMENT NUMBER

6. AUTHOR(S)
Heinz Pitsch

5d. PROJECT NUMBER

5e. TASK NUMBER

5f. WORK UNIT NUMBER

7. PERFORMING ORGANIZATION NAME(S) AND ADDRESS(ES)

Leland Stanford Junior
University
651 Serra Street
Stanford, CA 94305

8. PERFORMING ORGANIZATION REPORT NUMBER

9. SPONSORING / MONITORING AGENCY NAME(S) AND ADDRESS(ES)
AFOSR/NA
875 N Randolph St
Suite 325, Rm 3112
ARLINGTON, VA 22203-1768

10. SPONSOR/MONITOR'S ACRONYM(S)

11. SPONSOR/MONITOR'S REPORT NUMBER(S)

12. DISTRIBUTION / AVAILABILITY STATEMENT
Approved for public release; distribution is unlimited

13. SUPPLEMENTARY NOTES

14. ABSTRACT

In the present project the focus was on developing advanced combustion models for large-eddy simulations (LES) and to develop automatic chemistry reduction techniques and reduced chemical mechanisms for JP-8 surrogate fuels. The aim of the combustion LES modeling part was to advance the models for non-premixed and premixed combustion towards a generalized combustion model that covers all combustion regimes. Towards this end, for the premixed regime, a dynamic model for the turbulent burning velocity was developed, which eliminates adjustable coefficients from the premixed combustion model, and a flame structure model was presented, which considers local broadening of the flame preheat zone. Further, based on asymptotic arguments, a formalism to identify the correct combustion regime was developed, which will be an important element in a future generalized combustion-regime independent combustion model. In the second part of the project, several advancements led to a fully automatic chemistry reduction method. New developments include a refined DRGEP method for species and reaction elimination, a chemical lumping procedure, and an automatic procedure for selecting steady state species. Further, several potential surrogate fuel components have been included in the component library, and a reduced JP-8 surrogate mechanism was constructed and tested with experimental data.

15. SUBJECT TERMS
Turbulent combustion, Large Eddy Simulation, hydrocarbon fuels, reduced chemistry

16. SECURITY CLASSIFICATION OF:			17. LIMITATION OF ABSTRACT	18. NUMBER OF PAGES	19a. NAME OF RESPONSIBLE PERSON
a. REPORT	b. ABSTRACT	c. THIS PAGE			Julian M. Tishkoff
Unclassified	Unclassified	Unclassified	UL	41	19b. TELEPHONE NUMBER *(include area code)* (703) 696-8478

Chemical Modeling for Large-Eddy Simulation of Turbulent Combustion

Final Report submitted by:

Heinz Pitsch (PI)

Stanford University
Mechanical Engineering Department
Stanford, CA 94305-3030

Submitted to:

Dr. Julian M. Tishkoff
Air Force Office of Scientific Research
875 N Randolph St
Suite 325, Rm 3112
Arlington, VA 22203-1768

for the period:

November 15, 2005 through November 30, 2008

Contents

1 Sub-Grid Models for Large Eddy Simulation of Turbulent Combustion

1.1 Introduction

Large eddy simulation (LES) increasingly is being used to study turbulent reactive flows [1, 2, 3, 4]. While LES is computationally more expensive than ensemble averaged approaches, the resources that LES requires are applied in a particularly efficient manner. These resources are used to resolve the large energetic scales of turbulence. Large scale structures in general cannot be expected to remain statistically homogeneous, and ensemble averaged models, therefore, have difficulty describing them. In reactive flows in particular, large scale inhomogeneities are very important because they influence the mixing processes that affect the evolution of combustion.

The inherent resolution of the LES technique reduces the amount of work, relative to ensemble averaged techniques, that computational sub-grid models must perform. But the need for accurate sub-grid scale flow descriptions has not been eliminated. Rather, models that can account for the behavior of the smallest, unresolved turbulent scales remain fundamentally important. In spite of the significant progress that has been made in the field of LES, many questions regarding the large eddy simulation of reactive flows in particular still exist. Furthermore, although many sub-grid approaches for reacting flows have been proposed, universally accurate combustion models continue to remain elusive. Part I of this research project, therefore, sets the goal of analyzing and developing improvements to a set of the most promising sub-grid models for LES of turbulent combustion. These models are based primarily on asymptotic flamelet ideas that use single dimension chemistry solutions to describe multi-dimensional turbulent processes.

Although this mapping is difficult to perform accurately in itself, an additional difficulty is introduced when these asymptotic models have to be applied simultaneously to multi-regime combustors. In the following sections work will be presented both on individual asymptotic mapping methods and on how to combine these regime-specific methods appropriately in realistic device simulations. This work will be introduced through a brief review of the proposed project objectives.

1.1.1 Review of Objectives

Modern premixed turbulent combustion models are known to be subject to a number of deficiencies. For example, it is especially difficult to describe the propagation speed of turbulent premixed flames correctly, because flame propagation is highly dependent on what happens at the smallest, unresolved flow scales [5, 6]. Second, efforts to model underresolved premixed flames such as the level set approach often lead to inappropriate descriptions of premixed flame structure. These efforts consequently lead to incorrect descriptions of density being fed to a flow solver. The objective of the LES combustion modeling portion of this work was, therefore, to improve flame speed models and to lay the foundation for a

new flame structure model.

Work in the area of non-premixed turbulent combustion focused on improving models for the sub-grid variance of scalars. The variance of the mixture fraction scalar, in particular, is important in non-premixed combustion because the higher order moments of sub-grid mixture fraction distributions play a leading role in determining how combustion evolves. While both transport equation and dynamic algebraic variance models exist, this project focused on improving the dynamic procedure relevant for algebraic models. Algebraic models are used very widely, and improvements in this area, in turn, may help improve the modeling of unclosed terms in transport equation approaches.

Premixed and non-premixed behavior often both are observed in modern combustor designs [1, 7]. If the advantages of flamelet models are to be retained in these multi-regime environments, methods of selecting whether to map premixed or non-premixed chemistry solutions into a flow solver must be developed. Until recently, the flame index was the only available selection method. The flame index suffers from a number of drawbacks, however, such as its inattention to information regarding chemical time scales. Another objective of this work was, therefore, to develop an improved combustion regime index that would allow flamelet methods to be combined in multi-regime flows.

1.2 Premixed Turbulent Combustion

In typical large eddy simulations of premixed combustion, flame fronts exist on sub-grid length scales. Consequently, reactive scalar variables cannot be transported accurately. Specifically, the changes in density that occur at the flame front are resolved on only one or two mesh cells. These poorly resolved density changes lead to large numerical errors that affect the solution of all reactive scalar transport equations. The level set, or G-equation, premixed combustion model was proposed in response to this problem [6, 8]. This model, rather than resolving changes through the flame front, tracks the level set surface that describes the front.

The accuracy of level set based models is known to be particularly dependent on the numerical methods that are used. In response, a study of the accuracy of numerical level set methods in the context of premixed LES was conducted. A number of canonical level set test cases exist, and many of these have been used to validate the combustion models that are discussed below. The results of such tests, however, cannot be used readily to understand what happens in turbulent flow fields where front propagation is a multi-scale phenomenon. To overcome this problem, an adaptive mesh refinement technique, the Refined Level Set Grid (RLSG) approach, was implemented and applied to a turbulent flame.

In this technique, a secondary computational mesh is created locally around the flame front of interest. This mesh is resolved more highly than the baseline flow solver mesh and adapts to the flame front as it moves. The highly resolved mesh provides a means of transporting a significantly more accurate level set solution than the solution from the flow solver mesh. The influence of numerical error on the flame location can then be assessed by running with increasingly refined level set meshes.

If the numerical errors that occur when the level set is solved on the flow solver mesh are

significant, then the more accurate, refined flame solutions should display different characteristics. Additionally, the refined solutions should converge to the correct solution as the refined mesh resolution is increased. Application of the RLSG to a turbulent bunsen flame, however, showed that the flame front solution remained roughly constant as the resolution increased. Moreover, the solution differences that did appear were small in relation to the differences that developed as a function of heat release modeling choices. For example, an adjustment of the variance used in the probability density function (PDF) describing the likelihood of finding burned gas around the front impacted the flame location more than the level set mesh refinement did. The RLSG study, therefore, demonstrated that a level set framework was sufficiently numerically accurate to model turbulent premixed flames. While numerical errors were created, they were not the most dominant source of error. Attention was given, therefore, to modeling the turbulent burning velocity, premixed heat release, and flame structure.

1.2.1 Dynamic Turbulent Burning Velocity Model

Because of the poor flame resolution that is inherent in premixed LES, the propagtion speed of a flame front cannot even be captured moderately well by a filtered transported equation. This speed, therefore, has to be prescribed. A large variety of models for this propagation speed have been proposed, but most depend on a series of empirically defined coefficients [8, 9, 10]. In an effort to improve turbulent flame speed predictions, a dynamic procedure was developed for calculating these coefficients [5]. This procedure was formulated particularly to be consistent with the level set approach but could be modified easily to fit other models. By analogy to the dynamic Smagorinsky viscosity model, it was thought that a dynamic procedure that accounts for local information could describe how small scales influence front propagation more accurately. Another advantage of the dynamic procedure is that it limits the ability of model developers to affect flame behavior artificially through constant tuning.

The derivation of the dynamic turbulent burning velocity model begins by formulating an equation describing the evolution of a flame front. When a flame front is defined as an isocontour of a progress variable ($C = C_0$), the appropriate equation is produced by multiplying the progress variable transport equation with a delta function,

$$\delta\left(C - C_0\right)\left[\frac{\partial C}{\partial t} + u_j\frac{\partial C}{\partial x_j}\right] = \delta\left(C - C_0\right)\left[\frac{1}{\rho}\frac{\partial}{\partial x_j}\left(\rho\mathcal{D}_C\frac{\partial C}{\partial x_j}\right) + \frac{1}{\rho}\dot{\omega}_C\right]. \tag{1}$$

This delta function can be written equivalently as the derivative of a heaviside function, $\delta(C - C_0)\nabla C = \nabla[H\left(C - C_0\right)]$ and can be combined with the other terms in the transport equation. Some manipulation produces an expression describing the transport of a heaviside function located at the flame front,

$$\frac{\partial\left[H\left(C - C_0\right)\right]}{\partial t} + u_j\frac{\partial\left[H\left(C - C_0\right)\right]}{\partial x_j} = D\kappa|\nabla\left[H\left(C - C_0\right)\right]| + s_{L,C_0}|\nabla\left[H\left(C - C_0\right)\right]|, \tag{2}$$

where the propagation speed of the C_0 surface, s_{L,C_0}, has been introduced to account for the source terms. Unlike level set formulations, this equation is valid everywhere in space

and not just at the flame front surface. This property is important because it means that a standard LES volumetric filter can be applied to the equation. Making the notationally convenient substitution $\mathcal{G} = H(C - C_0)$ and then filtering gives

$$\frac{\partial \overline{\mathcal{G}}}{\partial t} + \overline{u_j \frac{\partial \mathcal{G}}{\partial x_j}} = \left(\overline{D\kappa}\right)_T \left|\nabla \overline{\mathcal{G}}\right| + \overline{s}_{T,C_0} \left|\nabla \overline{\mathcal{G}}\right|, \tag{3}$$

where

$$\overline{s}_{T,C_0} \left|\nabla \overline{\mathcal{G}}\right| = \overline{s_{L,C_0} |\nabla \mathcal{G}|}, \tag{4}$$

and

$$\left(\overline{D\kappa}\right)_T \left|\nabla \overline{\mathcal{G}}\right| = \overline{D\kappa |\nabla \mathcal{G}|}, \tag{5}$$

represent the introduction of definitions for the filtered burning velocity, $\overline{s}_{T,C_0}$, and the filtered propagation speed due to curvature, $\left(\overline{D\kappa}\right)_T$.

Equations (3)-(5) are significant because they can be used, after some further manipulation, to determine the form of the terms that the turbulent burning velocity describes explicitly. Additionally, when both filtering and test filtering are used, they provide the framework for producing a dynamic equation that can be solved to determine the value of turbulent burning velocity model coefficients. For example, since filters commute with temporal derivatives, the application of a broad test filter to Eq. (3) produces a transport equation for $\overrightarrow{\overline{\mathcal{G}}}$ (the arrow operator denotes the test filter). If a filter and a test filter instead are applied to Eq. (2) in a single operation, a different form of the $\overrightarrow{\overline{\mathcal{G}}}$ equation is realized. Because these two equations appear in different forms, they can be subtracted from one another to determine an expression relating turbulent burning velocity models associated with different filter widths. This expression can be written,

$$\overrightarrow{\left(\left(\overline{D\kappa}\right)_T + \frac{\rho_u}{\overline{\rho}} \overline{s}_{T,u}\right) \left|\nabla \overline{\mathcal{G}}\right|} = \left(\left(\overrightarrow{\overline{D\kappa}}\right)_T + \frac{\rho_u}{\overrightarrow{\overline{\rho}}} \overrightarrow{\overline{s}}_{T,u}\right) \left|\nabla \overrightarrow{\overline{\mathcal{G}}}\right|, \tag{6}$$

where the u subscript denotes that conditioning on the unburned side of the flame front is being considered. Once a specific model for $s_{\overline{T},u}$ is invoked, Eq. (6) can be solved locally in an LES to determine the value of a coefficient in that model [5].

Both $|\nabla \overline{\mathcal{G}}|$ and $|\nabla \overrightarrow{\overline{\mathcal{G}}}|$ are underresolved in actual LES computations. These terms, therefore, cannot be used directly in Eq. (6). An accurate method of approximating these terms based on information about the area of the filtered flame front has been developed in the last two reporting periods [5]. The physics behind this method are illustrated in Fig. 1, where a turbulent flame front is shown after having been filtered with increasingly wide filter kernels. As the filter width increases, the amount of small scale structures that remain grows smaller. The turbulent burning velocity, therefore, must increase to ensure that the flame front consumes the correct volume of unburned gas. This mass conservation criterion is accounted for inherently when filtered flame areas are used to represent $|\nabla \overline{\mathcal{G}}|$ in Eq. (4).

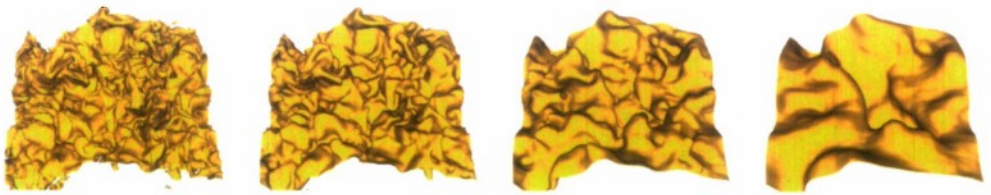

Figure 1: Filtered realizations of a turbulent flame front propagating at a speed of 2.5 times the integral scale velocity fluctuation. The realizations are filtered using kernels with widths of, from left to right, Δ/η = 0, 16, 32, and 64.

1.2.2 Turbulent Burning Velocity Model Performance

A direct numerical simulation (DNS) of a front propagating in forced homogeneous isotropic turbulence was performed to validate the dynamic turbulent burning velocity model. The DNS was computed on a 512×256×256 mesh at a Reynolds number of $Re_\lambda = 48$. The simulation was run at a constant density to isolate the propagation model from gas expansion effects. A level set was used to describe the flame front, and a laminar burning velocity of approximately one-third of the maximum velocity fluctuation magnitude was prescribed. An image from this simulation is shown in Figure 2.

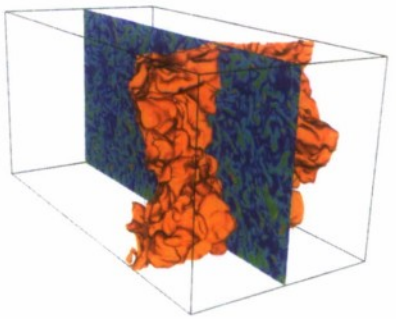

Figure 2: Snapshots from a DNS of front propagation. The level set is the wrinkled surface, and the cut plane shows voriticity magnitude.

The DNS was used to evaluate the filtered flame area model for the $|\nabla\overline{\mathcal{G}}|$ term in Eq. (4). The left hand side of Fig. 3 shows the time evolution of both the model and $|\nabla\overline{\mathcal{G}}|$ at a variety of filter resolutions. This plot demonstrates that the model accurately captures the gradients of the $\mathcal{G}$ variable as a function of time. The model performs well at all filter resolutions and correctly describes how the gradient fluctuations scale with filter width.

The right-hand side of Fig. 3 shows the performance of the proposed dynamic turbulent burning velocity model at three canonical filter combinations. The filter width $\Delta/\eta = 5$ is the case that is most representative of an LES, and in this case the dynamic model performs much better than the model in which a constant coefficient is used. The $\Delta/\eta = 2$ case does not represent a realistic LES, but it does serve to verify that the model correctly asymptotes to a fully resolved limit when the filter width becomes small. Many constant coefficient LES models do not correctly describe the burning velocity as this limit is approached. Finally, the case in which $\Delta/\eta = 256$ demonstrates that the model performance break downs for certain sets of conditions. These conditions occur when the assumed form of the $s_{\overline{T},u}$ expression that is used in Eq. (6) is overtaxed. This limiting case will need to be addressed in future work.

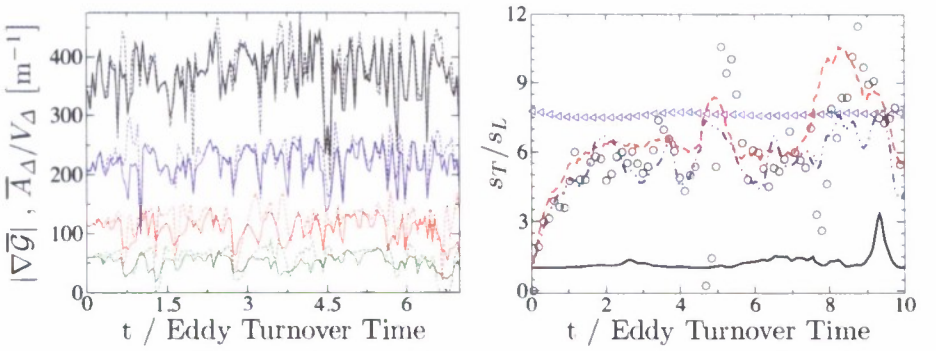

Figure 3: Left: Time history of $|\nabla\overline{\mathcal{G}}|$ (——) and of the filtered flame area per filter volume $\overline{A}_\Delta/V_\Delta$ (- - - -) in the DNS. From top (black) to bottom (green), the filter width is $\Delta/\eta = 4$, 8, 16, and 32. Right: Time history of $s_{\overline{T},u}$, from: DNS data (∘∘), Constant coefficient model (◁◁), Dynamic model with: $\Delta/\eta = 2$ and $\Delta'/\eta = 512$ (– ·· –), $\Delta/\eta = 5$ and $\Delta'/\eta = 10$ (- - - -), $\Delta/\eta = 256$ and $\Delta'/\eta = 512$ (——).

The dynamic turbulent burning velocity model also was applied in an LES of a piloted turbulent bunsen flame. A schematic of this LES is shown in Fig. 4. The contour cut plane shows the temperature field, while the isocontour shows the level set that represents the flame front. The level set is colored by the ratio of the filtered and test filtered flame front areas that are used to compute the $|\nabla\overline{\mathcal{G}}|$ terms in Eqs. (4) and (6). This ratio is spatially dependent, and this dependence is introduced to the flame speed through the dynamic coefficient calculation.

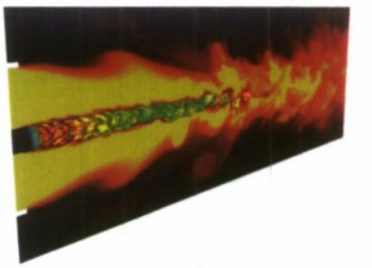

Figure 4: Instantaneous snapshot from an LES of the F3 flame. The cut plane shows a contour plot of temperature, which ranges from 300 K (black) to 2200 K (bright yellow). The premixed flame front is colored according to the ratio of the filtered and test filtered flame areas.

Figure 5 shows that the use of the dynamic procedure strongly affects the predicted burning velocities. The left plot in the figure shows the predicted LES burning velocity when a constant model coefficient (α) is used. The right plot shows the predicted burning velocity when the coefficient is calculated using a dynamic procedure. In this LES, the dynamic model reduces the magnitude of the turbulent burning velocity by as much as 50% of the laminar burning velocity $s_{L,u}$. This reduction can be attributed to the dynamic model's recognition of the relatively high resolution of the LES. The differences between the dynamic and constant coefficient models emphasize the importance of accounting for local filtered physics in LES combustion models.

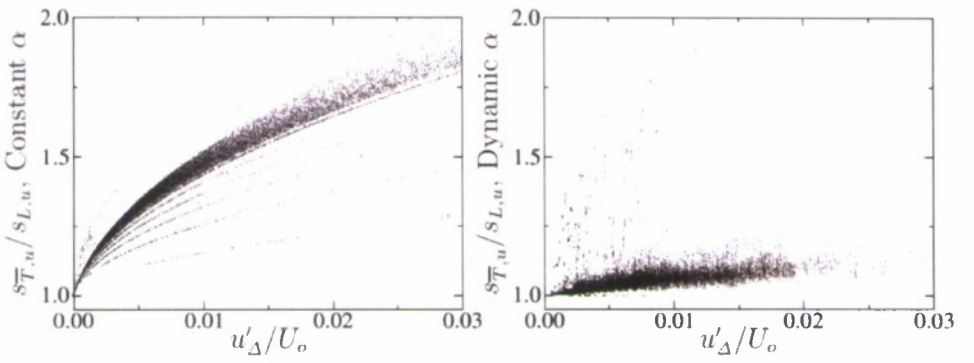

Figure 5: Instantaneous scatter plots of the turbulent burning velocity as a function of turbulent velocity fluctuations in the bunsen flame LES. Left: $s_{\overline{T},u}$ is computed using a constant value of the model coefficient α. Right: $s_{\overline{T},u}$ is computed locally in the LES using a dynamically determined value of α.

1.2.3 Flame Structure Model

Level set models are advantageous because they describe flame front propagation at arbitrary mesh resolutions without altering how turbulence affects the front, but they have one inherent drawback. Because a level set represents a 2-D surface, it cannot be used to describe the interior structure of a premixed flame. A field quantity such as a progress variable also must be considered if this interior structure is to be described accurately, but the only way to protect a progress variable equation from numerical errors in premixed combustion is to couple it to a level set at the flame front. In response to this problem, a coupling procedure was developed that can describe 3-D flame structure and account correctly for flame propagation using level sets.

The level set and progress variable coupling is performed by making the source term in a progress variable ($\widetilde{C}$) transport equation dependent on the location of a level set [11]. This dependency is introduced by assuming that the unfiltered C variable can be written as a presumed function of a distance coordinate (F in this context), and that $\dot{\omega}_C$ can be written as a presumed function of C. A 1-D flame structure is assumed additionally, and the $\dot{\omega}_C(C(F))$ function then can be integrated against a filter kernel to find an analytical expression,

$$\overline{\dot{\omega}}_C(\widetilde{C},\widehat{F},\Delta) = \int_{-\infty}^{\infty} \left\langle \dot{\omega}'_C | \widehat{F}=F,\widetilde{C} \right\rangle \overline{P}\,(F,\mathbf{x},t,\Delta)\,dF, \tag{7}$$

where $\left\langle \dot{\omega}_C | \widehat{F}=F,\widetilde{C} \right\rangle$ is the conditional average of $\dot{\omega}_C$ along a surface that is a distance $\widehat{F}=F$ away from the filtered flame front position. $\overline{P}\,(F,\mathbf{x},t,\Delta)$ is the PDF that describes the likelihood of the location $\mathbf{x}$ being a distance F away from the front. Figure 6 shows a schematic of the new model.

The PDF in Eq. (7) couples the progress variable to the level set and is easy to compute. The conditioned source term in Eq. (7) represents more of a challenge but can be described

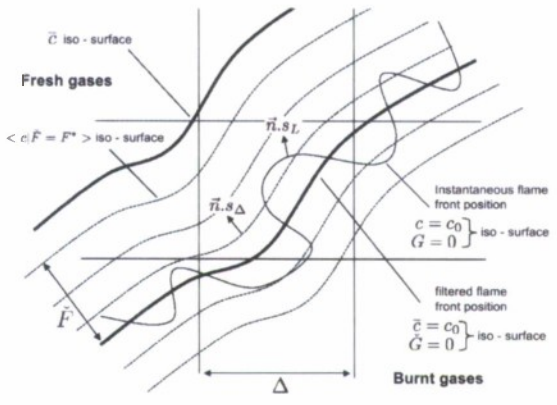

Figure 6: The flame structure model.

using a variety of chemical models. This approach led to excellent predictions of the behavior of a bluff-body-stabilized premixed flame [11]. The flame burned in the thin reaction zones regime, which was an appropriate validation test since, in this regime, turbulence tends to thicken premixed flame structures. In future work, this model will be developed further to work in conjunction with standard tabulated chemistry models such as the Flamelet Progress Variable approach.

1.3 Partially Premixed Turbulent Combustion

Although premixed and non-premixed flamelet solutions can be mapped cheaply and effectively into turbulent flows, these mapping approaches become problematic when partially premixed or multi-regime combustion environments are encountered. In these environments, it becomes unclear whether a premixed, a non-premixed, or an auto-ignition chemical solution should be used to describe chemistry. For example, when fuel is injected into a device by means of a liquid spray, local evaporation and mixing rates might lead to either premixed or non-premixed conditions. Consequently, methods of dealing with multi-regime and partially premixed combustion in flamelet-based LES should be considered.

The flame index proposed by Yamashita *et al.* [12] is one of the only available indicators from the literature that can be used to determine combustion regimes. The flame index simply examines whether or not gradients of oxidizer and fuel align and then sets the local regime accordingly [12, 13, 14]. This index is based, however, on 1-D geometric arguments, and the extent to which it can be applied to fully 3-D turbulent flames is not yet known. For example, in certain flow settings gradients of fuel and oxidizer do align, but combustion nonetheless remains diffusion-controlled. The flame index does not capture the physics that are relevant in these regimes [14].

1.3.1 Combustion Regime Indicator Formulation

A new Combustion Regime Indicator (CRI) model has been developed in an effort to capture more of the physics that determine local burning modes. The indicator itself can be derived using a generalized flamelet-type transformation of variables. The mixture fraction, Z, is

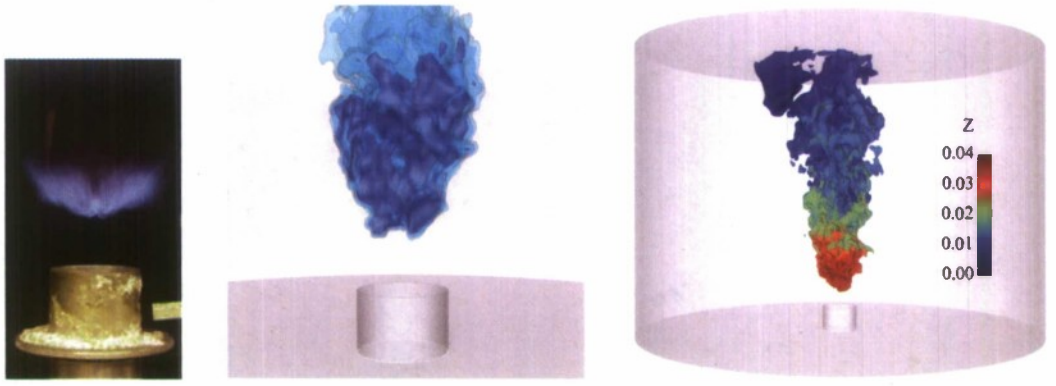

Figure 7: Instantaneous fields from the swirl burner. Left: Typical LSB experimental image, from Cheng [15, 16]; Middle: Three $\widetilde{C}$ isocontours from the LES; Right: LES level set representation of the flame front, colored by $\widetilde{Z}$;

retained as one of the transformation coordinates because it describes the asymptotic non-premixed regime. The key insight provided by the indicator lies in the second transformation coordinate, which must describe combustion in the asymptotic premixed regime and be statistically independent of Z. A flamelet variable Λ that satisfies these requirements can be defined as the value of the progress variable C that occurs at a stoichiometric mixture fraction ($Z = Z_{\text{st}}$) on a given flamelet. When the scalar transport equation for a reacting chemical species is transformed into Z and Λ space, the transformed terms can be grouped according to the asymptotic regime in which they appear. The transformation takes the form

$$\begin{aligned} &\Big(\rho\partial_\tau C + \partial_\Lambda C\left[\rho\partial_t\Lambda + (\rho\mathbf{u} - \rho_u s_{L,u}\mathbf{n})\cdot\nabla\Lambda\right]\Big)_1 \\ &+ \Big(\partial_\Lambda C\left[\rho_u s_{L,u}|\nabla\Lambda| - \nabla\cdot(\rho\mathcal{D}_C\nabla\Lambda)\right] - \rho\frac{\chi_\Lambda}{2}\partial_\Lambda^2 C\Big)_2 \\ &+ \Big(-\rho\frac{\chi_Z}{2}\partial_Z^2 C\Big)_3 = \dot{\omega}_C, \end{aligned} \tag{8}$$

where group 1 terms describe unsteady combustion, group 2 terms describe premixed combustion, and group 3 terms describe non-premixed combustion. These terms then can be evaluated in a simulation and compared to one another to determine which asymptotic group of terms balances a local chemical source term. This balance indicates the regime in which a flame burns.

1.3.2 Model Application: LES of a Low Swirl Burner

The CRI has been tested in an LES of the low swirl burner shown in Fig. 7. This burner has been the subject of previous experimental and computational investigations [4, 16, 17] and is particularly interesting to investigate from the standpoint of regime prediction.

Regime predictions are interesting because the coflowing air in the burner mixes with the primary premixed fuel stream and changes the nature of the combustion regime along the downstream direction. Figure 7 shows two images from the LES, in which the CRI has been used actively to apply asymptotic combustion solutions [1]. In particular, the right plot indicates how the coflowing air leans out the primary fuel stream. The level set isocontour that is shown in this plot is colored by mixture fraction, which steadily decreases between the nozzle and the burner exit. The left two plots in this figure show that the flame predicted by the CRI methodology instantaneously compares well to a typical experimental visualization of the burner.

Figure 8 shows time-averaged profiles from the centerline of the burner. The mean axial velocity is shown along with the mean and rms temperatures as a function of the burner axial coordinate. This figure is particularly noteworthy because it demonstrates that the central flow feature of the swirl burner is captured accurately by the LES. This feature is the linearly decreasing centerline axial velocity profile. The decrease in axial velocity is created by the recirculation region that the swirling flow sets up. The decreasing velocity profile acts to stabilize the position of the burner's premixed flame. The figure shows that the LES temperature profiles are in especially good agreement with the experiments. The agreement suggests that the combustion model is performing well, and that the CRI and generalized flamelet transformation theory can be applied consistently in LES.

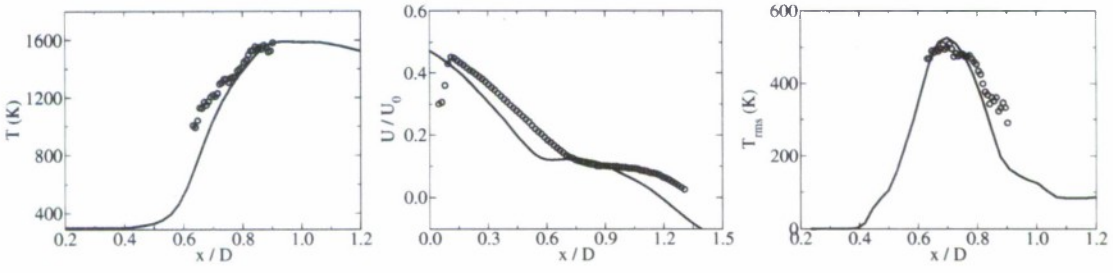

Figure 8: Time averaged swirl burner centerline profiles. LES solutions (——); Experimentally measured profiles (o o o) [17]. Axial velocity, axial RMS velocity, temperature, and RMS temperature are shown as a function of downstream displacement along the burner centerline.

2 Development of an Interactive Platform for Generation, Comparison, and Evaluation of Kinetic Models for JP-8 Surrogate Fuels

2.1 Introduction

Cost and efficiency drive the design of combustion devices to rely more and more on numerical simulations. As the methods for computational fluid dynamics (CFD) progress, complex problems such as the simulation of chemically reactive flows in engines become tractable. Of interest, for instance, is the capability to predict accurately pollutant emissions from engines, such as particulate matter, carbon monoxide CO, and oxides of nitrogen NO_x, all contributing at different levels to the greenhouse effect and global warming, smog, ground-level ozone, stratospheric ozone depletion, and a myriad of related health problems. To predict and control these emissions, the understanding and the accurate modeling of chemistry is tremendously important. Currently, petroleum-derived fuels make up a very large portion of our energy resources, and their combustion proceeds through complex highly non-linear processes involving hundreds of different chemical compounds; therefore, a detailed chemical modeling of real hydrocarbon fuels is excluded, and the fuel representation needs to be simplified drastically to be included in numerical simulations of combustion devices.

A first stage of simplification consists of approximating the fuel by a well-defined mixture of a few components (surrogate fuels) that will match some physical or chemical properties of the real fuel. Using surrogate fuels in lieu of real fuels presents numerous advantages, among which are the reproducibility of experiments and the possibility of formulating chemical models suitable for CFD, but even with this simplification, deriving chemical models for surrogate fuels that can be used in CFD simulations remains a real challenge for many reasons. First, hydrocarbon fuels obtained through crude oil refining processes are required to satisfy a number of physical or chemical criteria that sometimes are formulated only loosely; therefore, their composition can vary significantly among feed-stocks, and at best, only average fuel properties are known. Then comes the question of how to define the surrogate compositions. Guidelines and targets have to be developed to select appropriate individual components and their respective contribution to the surrogate mixture. Chemical modeling for these surrogates is a major challenge as well. State-of-the-art detailed kinetic models can comprise on the order of a thousand different species and several thousand reactions, even for single components. Uncertainties in kinetic data mean that chemical mechanisms from different sources will represent similar reaction pathways differently, rendering the merging of detailed mechanisms to create multi-component mechanisms extremely difficult. Additional complications come from the fact that chemical modeling of single components and fuel surrogate compositions likely will evolve, and previously derived models will become obsolete. Finally, current computational resources and numerical combustion models put severe restriction of the size and detail allowable for the chemistry. Detailed chemical models must be reduced considerably in size before their implementation in CFD codes can

be considered.

2.1.1 Review of Objectives

The present effort aims to provide some solutions to the issues raised above. The work is organized around two major axes: an efficient chemical reduction strategy and a systematic, modular approach to derive surrogate chemical models. The former is crucial to incorporate a certain level of detail in the combustion models of CFD codes, while flexibility and consistency appear essential to go beyond the current empirical stage of the surrogate fuel approach.

A previous AFOSR-funded project led to the development of the Directed Relation Graph with Error Propagation (DRGEP) reduction method, which automatically eliminates from a kinetic mechanism the species and reactions that do not contribute significantly to the overall dynamics of a chemical process; however, this single approach showed limitations, especially in the case of kinetic mechanisms involving a large number of branched species. The first objective of the present work, therefore, is to improve the DRGEP method and complement it with additional reduction strategies such as a chemical lumping method and the automatic introduction of simplifying assumptions such as quasi-steady states.

The next objective is the development of a modular framework, called the component library approach, to formulate surrogate compositions optimized for a given application and specific hydrocarbon fuel automatically, and generate validated multi-component reduced models for these surrogates. Emphasis is placed on developing reduced models for JP-8. To achieve this goal, a preliminary version of the component library developed under our previous AFOSR grant needed to be extended to include compounds relevant to jet fuels, such as long-chain alkanes, cyclo-alkanes, and aromatic components. To obtain the smallest possible kinetic models, the potential of a modular approach was explored, in which modules describing for example low-temperature ignition or soot formation were developed and included in the surrogate kinetic models only if necessary. Finally, the viability of the overall surrogate modeling strategy needed to be assessed through the development of a reduced jet fuel surrogate model.

2.2 Automatic Reduction of Detailed Chemical Kinetic Mechanisms

Three different reduction techniques have been developed, each of them addressing a different aspect of kinetic reduction. The first one, called Directed Relation Graph with Error Propagation (DRGEP) method, eliminates species and reactions [18], the second one compacts information through chemical isomer lumping [19], and the third one introduces quasi-steady state assumptions using a criterion based on lifetime analysis and DRGEP [20]. The different techniques are combined into an integrated approach that is shown to reduce drastically the size of large-scale kinetic mechanisms.

2.2.1 Elimination Stage: The Directed Relation Graph with Error Propagation Method

The goal of the elimination stage is to identify, for any number of species in the skeletal mechanism, N_{skel}, a group of species of size $N_{\text{rm}} = N_{\text{det}} - N_{\text{skel}}$ that can be removed with minimal impact on the targets. The choice of these species is done here by defining appropriate importance coefficients for each species based on the production and consumption rates, which are evaluated using results obtained from the detailed mechanism. The species with the N_{rm} lowest importance coefficients are removed from the mechanism, and a skeletal mechanism of size N_{skel} is created by removing from the detailed mechanism any reaction in which a removed species appears as a reactant or as a product.

Direct interaction coefficients Direct interaction coefficients are defined as the measure of the coupling between two species that are related directly through an elementary reaction, that is, two species that appear concurrently in the same reaction. In the DRGEP method, the coupling coefficient between two directly related species A and B is estimated as follows:

$$r_{AB} \equiv \frac{\left|\sum_{i=1,n_R} \nu_{i,A}\omega_i\delta_B^i\right|}{\max\left(P_A, C_A\right)}, \tag{9}$$

where

$$P_A = \sum_{i=1,n_R} \max\left(0, \nu_{i,A}\omega_i\right), \qquad \text{and} \qquad C_A = \sum_{i=1,n_R} \max\left(0, -\nu_{i,A}\omega_i\right). \tag{10}$$

Equation (9) provides an estimate of the impact that removing one species has on the calculated concentration of the remaining species; however, the goal of the reduction procedure is to remove the largest possible set of species from the mechanism while keeping errors below a given tolerance. Considering one species independently of the group of removed species in which it will belong eventually might lead to a very inaccurate estimate of the importance of each species. This observation leads to the extension of Eq. (9) given a set of removed species:

$$r_{AB,\{\mathcal{S}\}} \equiv \frac{\left|\sum_{i=1,n_R} \nu_{i,A}\omega_i\delta_{B,\{\mathcal{S}\}}^i\right|}{\max\left(P_A, C_A\right)}, \tag{11}$$

where $\{\mathcal{S}\}$ is the set of species already removed. $\delta_{B,\{\mathcal{S}\}}^i$ is unity, if the i^{th} reaction involves B or any species in subset $\{\mathcal{S}\}$, and 0 otherwise.

Error Propagation The goal of the elimination stage is to remove species and reactions that negligibly impact a user-defined set of targets. Intuitively, the farther away from the target a species is, the smaller the effect of changing or removing this species should be. To reflect this error propagation effect, a geometric damping has been introduced in the

selection procedure; therefore, we define a path-dependent coefficient:

$$r_{AB,p} = \prod_{i=1}^{n-1} r_{S_i S_{i+1}}, \tag{12}$$

and a global importance coefficient

$$R_{AB} \equiv \max_{\text{all paths } p} r_{AB,p}. \tag{13}$$

If some error is introduced in the prediction of a species B, the longer the way this error has to propagate to reach the target A, the smaller its effect will be typically. This technique is target-oriented and is expected to provide a finer selection of the chemical paths necessary for the accurate prediction of the set of targets by keeping species associated with large R coefficients and discarding species with small R coefficients. A similar procedure is adopted to reduce the number of reactions [18].

Integrity Check Every intermediate species in a skeletal mechanism must have at least one production and one consumption path. During the DRGEP reduction process, some species might fail this requirement, especially for high reduction ratios in the context of complex, highly non-linear kinetic schemes. Two basic observations can be made. In a closed system, any intermediate species that is not produced anymore remains at its initial zero concentration and can be removed from the mechanism. On the other hand, if a species is produced, but not consumed anymore, it creates a sink of mass that may impact greatly the final concentration of the products. This complex non-linear behavior cannot be detected by a method based solely on the analysis of the detailed production rates; therefore, a simple algorithm has been designed to prevent these situations from occurring. A list of species, sorted by order of importance for the targets, is obtained first by computing the DRGEP coefficients using Eq. (9). Then this list is modified slightly so that, for any value of the cutoff parameter, the group of species kept in the skeletal mechanism forms a consistent chemical scheme with no truncated paths.

Validation Before applying the above reduction methodology, the validity of the error propagation assumption in the DRGEP method needs to be appraised. This assumption states that the effect on a target introduced by the removal of a species can be approximated through geometric damping along the directed relation graph, from the target to the removed species, which can be written as

$$E_{\mathrm{T}} \propto \mathrm{R}_{\mathrm{TS}}, \tag{14}$$

where E_{T} is the error between the prediction of the target using the detailed and skeletal mechanisms and R_{TS} measures the importance of a species S with respect to the target, as defined by Eqs. (9) and (13). This proportionality can be verified *a posteriori* using a practical case. The coefficients R_{TS} were computed for the adiabatic, isochoric auto-ignition of

a stoichiometric mixture of iso-octane and air at 13 bar and 1000 K, with iso-octane as the only target. The mechanism used for the simulation was the iso-octane oxidation scheme of Curran et al. [21]. Figure 9 shows the correlation between this error and the computed coefficients obtained using error propagation. For comparison, the correlation between the error and the coefficients obtained without error propagation is shown also in the same figure. The solid line represents the optimal case, that is, a hypothetical parameter whose value would be exactly equal to the error introduced if the species were removed. The

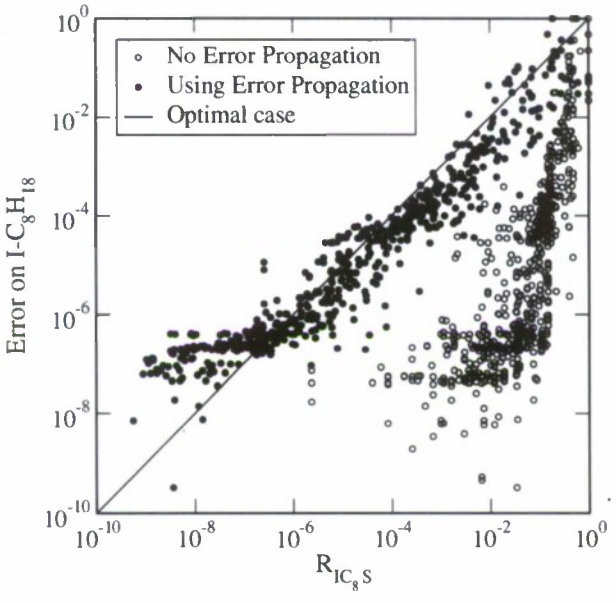

Figure 9: Correlation between the error introduced in the fuel prediction and the species coefficients R_{IC_8} s obtained with and without error propagation during the isochor, adiabatic auto-ignition of a stoichiometric mixture of iso-octane and air at 13 bar and 1000 K.

errors introduced by removing individual species correlate extremely well with the error propagation coefficients, with a small scatter in the data, whereas the correlation is not as obvious without error propagation. Figure 9 also shows that the error propagation method leads to an order unity coefficient in Eq. (14). This observation means that the importance coefficients evaluated by DRGEP are a direct measure of the error in the resulting mechanism.

The efficiency of the group-based coefficients and the integrity check are illustrated next. The detailed mechanism for iso-octane oxidation from Curran et al. [21] is reduced for a single initial physical condition, the homogeneous, adiabatic auto-ignition at constant volume of a stoichiometric mixture of iso-octane and air at an initial pressure of 13 bar and an initial temperature of 625 K. The targets are fuel, CO, CO_2, and temperature. Figure 10 shows the evolution of the error in ignition delay time and in the final mass fraction of carbon monoxide as functions of the number of species kept in the skeletal mechanism. When the definition of Eq. (9) is used, the error in the final mass fraction of CO in the system quickly

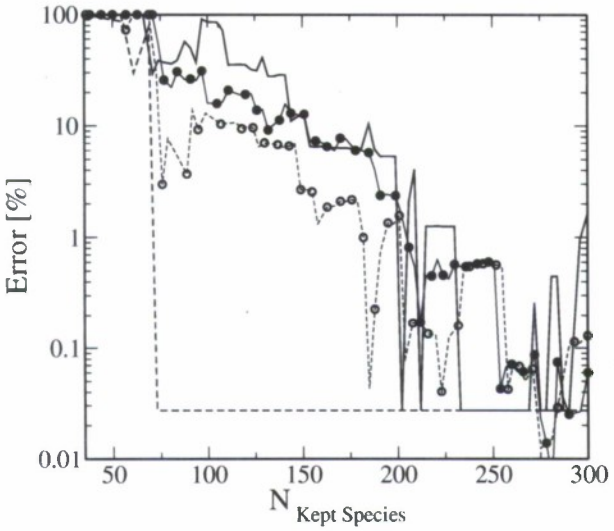

Figure 10: Iso-octane auto-ignition at low temperature. Evolution of the error in ignition delay time (lines with symbols) and final mass fraction of CO (plain lines) when the group-based coefficients and the integrity check algorithm are used (open symbols, dashed lines) or not (filled symbols, solid lines).

reaches a few percent and keeps increasing. This behavior is due to truncated chemical paths appearing as species are removed. Carbon mass accumulates in large quantities in intermediate species, which shifts considerably the chemical equilibrium of the system. When group-based coefficients and integrity check are included in the reduction process (the coefficients are recomputed once every 50 species removed), the error in the final mass fraction of CO remains extremely small, and the error in ignition delay time is improved considerably.

To demonstrate the full capabilities of the DRGEP method, the same very large mechanism for iso-octane oxidation [21] is reduced for adiabatic auto-ignition at constant volume over a large range of initial conditions relevant for engine-related applications (ignition delay times less than one second). The initial conditions include equivalence ratios between 0.5 and 2, pressures between 1 bar and 40 bar, and temperatures between 600 K and 1500 K. The detailed mechanism comprises 850 species and 7212 reactions. Targets for the reduction are fuel i-C_8H_{18}, major products CO and CO_2, and temperature. The DRGEP coefficients for temperature are evaluated using heat release data. Overall, errors are shown to increase monotonically as the number of species is reduced. The total number of species kept in the skeletal mechanism is chosen so that the maximum error over all targets is about 15%, which corresponds to 196 remaining species and 1762 remaining reactions, forward and backward counted separately. Following this first step of reduction and with the same accuracy requirement, additional non-necessary reactions are removed, and the resulting skeletal mechanism comprises 195 species and 802 reactions, that is, a reduction by a factor of 4.35 of the number of species and a reduction by a factor of 9 of the number of reactions. Table 1 provides an estimate of the error introduced in ignition delay times over the entire

reduction domain by this first stage of reduction.

N_{Species}	$N_{\text{Reactions}}$	Maximum Error [%]	Average Error [%]
196	1762	15.89	6.02
195	802	14.96	5.55

Table 1: Maximum and average errors introduced by the elimination stage of reduction, for initial conditions with pressures between 1 and 40 bar, equivalence ratios between 0.5 and 2, and temperatures between 600 K and 1500 K.

2.2.2 Compacting Stage: A Chemical Lumping Approach

A second important aspect of kinetic reduction aims at describing the system in terms of a reduced number of variables, called lumped variables, through a linear or non-linear transformation. In the present work, a general automatic lumping approach was derived that directly uses simulation results obtained from the detailed mechanism to generate a lumped scheme valid over a user-specified range of conditions. The method, applied here to isomer lumping in hydrocarbon oxidation kinetic schemes, does not rely on equilibrium or quasi- steady state assumptions. In addition, the resulting lumped mechanisms are suitable for direct use in standard chemistry software. In the following, the proposed lumping procedure will be detailed briefly, and the quality of the resulting lumped schemes will be assessed.

Proposed Modeling Approach Suppose the original set of species $\mathcal{S} = \{S_{i,i=1..N_S}\}$ is sub-divided into $\widetilde{N}_S$ lumped groups $\mathcal{L}^S_{I,I=1..\widetilde{N}_S}$. For each lumped group $\mathcal{L}^S_I$, a representative species is defined as a linear combination of the species of this group, such that:

$$\left[\widetilde{S}_I\right] = \sum_{i \in \mathcal{L}^S_I} [S_i] \,. \tag{15}$$

We define the relative contribution of species S_i to its group as:

$$\alpha_i = \frac{[S_i]}{\left[\widetilde{S}_I\right]} \,. \tag{16}$$

The reaction rate of a reaction j can be expressed using the lumped variables:

$$\omega_j = k_j \prod_{i=1}^{N_S} \alpha_i^{\nu'_{i,j}} \prod_{I=1}^{\widetilde{N}_S} \left[\widetilde{S}_I\right]^{\widetilde{\nu}'_{I,j}} \,. \tag{17}$$

where $\widetilde{\nu}'_{I,j} = \sum_{i \in \mathcal{L}^S_I} \nu'_{i,j}$. At this stage, the reactions that have become identical after the lumping of species also can be lumped together, the rate of each lumped reaction being

defined as:

$$\widetilde{\omega}_J = \sum_{j \in \mathcal{L}_J^R} \omega_j = \widetilde{k}_J \prod_{I=1}^{\widetilde{N}_S} \left[\widetilde{S}_I\right]^{\widetilde{\nu}'_{I,J}}, \quad \text{with} \quad \widetilde{k}_J = \sum_{j \in \mathcal{L}_J^R} \left(k_j \prod_{i=1}^{N_S} \alpha_i^{\nu'_{i,j}} \right). \tag{18}$$

This transformation corresponds to an exact linear lumping if $\widetilde{k}_{J,J=1..\widetilde{N}_R}$, and, therefore, the relative contributions $\alpha_{i,i=1..N_S}$, are known functions of time and space. Unfortunately, these functions usually are unknown, and a closed form has to be assumed. In this work, rather than specifying the relative distributions as functions of physical space and time, models for these distributions will be formulated in terms of the state space:

$$\left\{T, P, \left[\widetilde{S}_I\right]_{I=1..\widetilde{N}_S}\right\}. \tag{19}$$

Suppose that a subset Π of the state space variables is chosen to parameterize a set of data σ. In our case, σ refers to the relative distributions $\alpha_{i,i=1..N_S}$ or to the lumped rates $\widetilde{k}_{J,J=1..\widetilde{N}_R}$. In most cases, no explicit relationship between the data and the chosen state parameters can be found; therefore, a model $f^\sigma(\Pi)$ has to be formulated that will approximate the actual data by a function of the parameters included in Π. Both the choice of the set of parameters and the definition of the function f will impact the quality of the model.

A promising approach is to use non-linear data modeling tools such as artificial neural networks, which can be seen as parametric functions whose weights are adjusted by training the network to minimize errors [22]. This technique retains the dependence of the data on a large number of state variables, thus introducing very little error in the model; however, the training process is not an easy and straightforward procedure, and the resulting mechanism would not be used easily in standard chemistry packages, such as the Chemkin libraries, as extra routines need to be provided to evaluate the lumped rate constants; therefore, for practical reasons, the approach will be demonstrated and analyzed by considering only constant values or temperature dependent values of α_i. To increase accuracy, the modeling procedure will be applied directly to the lumped rate coefficients $\widetilde{k}_J$ instead of the relative contributions α_i. Then, the lumped rate coefficients can be expressed in Arrhenius form and the lumped reactions incorporated readily into the lumped mechanism that retains the same format as the detailed mechanism. Accordingly, $\widetilde{k}_J$ will be modeled using a basis function of the form:

$$f^{\widetilde{k}_J}(T) = \beta T^\gamma e^{-\frac{\delta}{RT}}. \tag{20}$$

The determination of the unknown coefficients β, γ, and δ is done using the detailed simulation data. To illustrate the soundness of this simplifying assumption, the data for the iso-octyl isomers obtained using the mechanism of Curran et al. [21] are projected onto the temperature and shown in Fig. 11. The role played by these isomers in the overall dynamics of the system might be more or less important depending on the configurations. A global interaction coefficient was defined as part of the DRGEP methodology presented in [23]

that quantifies the impact of a species on major parameters such as ignition delay time, laminar burning velocities, or fuel consumption. This DRGEP coefficient R is computed for all cases and used as a weighting factor to analyze the relative contribution of each iso-octyl isomer. In Fig. 11, darker colors mean larger coefficients R, that is, a higher importance of the radicals in the mechanism. These data demonstrate that keeping only the temperature

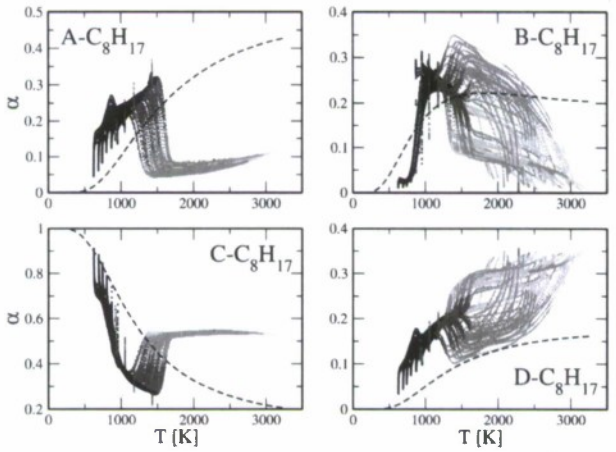

Figure 11: Iso-octyl radical distribution as function of the temperature for homogeneous and flame configurations. Darker colors mean higher DRGEP coefficients. Dashed lines correspond to thermodynamic equilibrium ratios.

dependence of the distribution functions α is a good approximation at low temperatures, whereas some scatter is observed at higher temperatures; however, less accuracy in the isomers distribution will have little impact on the prediction of the targets, as indicated by smaller DRGEP coefficients. Also shown in Fig. 11 are the relative contributions computed using the equilibrium constants of the isomerization reactions. Although the trends are similar, using the pseudo-equilibrium assumption to evaluate α might introduce large inaccuracies in the reaction rates.

To maintain high accuracy in hydrocarbon oxidation mechanisms, the overall organization of the detailed mechanism should be kept in the lumped mechanism. For example, representative elementary steps of each specific class of reaction should be present regardless of the extent of reduction. The presence of these elementary steps allows the reduced mechanism to be used to get insight into the dynamic chemical processes occurring during combustion. A simple way to achieve this result, which is followed here, is to lump together chemical isomers, as these species have potentially similar formation and decomposition pathways. Additionally, for some groups of isomers, taking into account the size of the ring in the transition states, as suggested by Ahmed et al. [24], improved results dramatically, with a small loss in the degree of reduction.

Results and Validation The skeletal mechanism for iso-octane oxidation obtained through species and reaction elimination [23] is used as a starting mechanism to demonstrate the

efficiency of the lumping approach. This mechanism contains 195 species and 802 reactions, backward and forward reactions being counted separately. Among those species, 27 lumped groups involving 88 chemical isomer species can be identified, leading to a reduction of the number of species from 195 to 135 if all groups of isomers are lumped and a reduction of the number of reactions to 611.

In addition to the auto-ignition configurations used to generate Fig. 11, the lumped mechanism obtained above with the proposed method was used to simulate atmospheric plug flow reactors modeled by isobaric homogeneous systems, and atmospheric one-dimensional laminar premixed flames. Table 2 provides the errors obtained over all conditions between skeletal and lumped schemes for ignition delay times and laminar burning velocities, which are two parameters describing the global behavior of the considered systems. Virtually no error on the final concentration of the products was observed. The small errors show that the

Error in τ_{ig} [%]	Max	16.19
	Avg	4.75
Error in S_L [%]	Max	1.05
	Avg	0.67

Table 2: Comparison of global parameters between skeletal and lumped iso-octane mechanisms.

prediction of global parameters is quite accurate. More remarkably, even though the lumped rate coefficients were modeled using homogeneous reactor data only, the resulting scheme is applicable to different configurations such as flames; however, additional comparisons are required to ensure that the lumping does not affect fundamental aspects of the original mechanism, for example, mass fluxes between species. The adequate representation of a group of isomers can be assessed by comparing the sum of the concentration of isomers of the lumped group to the actual concentration of the representative species. For an accurate lumping, these two quantities should be equal, as indicated by the fundamental definition of the representative species in Eq. (15). This property is demonstrated in Fig. 12 for the iso-octane lumped mechanism for an auto-ignition case, which shows that the concentration of the representative octyl radical compares very well to the sum of the four octyl radicals lumped together.

2.2.3 Introduction of Modeling Assumptions: The Quasi-Steady State Approximation

To increase the speed up of the skeletal mechanism obtained through species and reaction elimination and chemical lumping even further, a straightforward strategy is the introduction of quasi-steady state assumptions that replace part of the differential equations by algebraic equations, which are much faster to evaluate. In the present work, suitable QSS species are identified systematically through the evaluation of a steady-state parameter based on lifetime analysis and DRGEP coefficients [18]. The steady state parameter for a

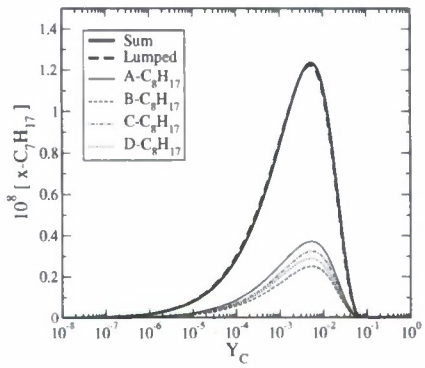

Figure 12: Comparison of iso-octyl isomers and lumped representative species concentrations during auto-ignition.

species S can be expressed as:

$$Q_S(t) = \alpha_T R_{TS}[S]\tau_S\,, \tag{21}$$

where $[S]$ is the concentration of species S and the lifetime of this species can be expressed in terms of its production and consumption rates

$$\tau_S = -\left[\frac{\partial\left(P_S - C_S\right)}{\partial\left[S\right]}\right]^{-1}. \tag{22}$$

The species with small Q values for all cases can be set in steady state. For simplicity, only linear coupling between steady state species is allowed, so that explicit expressions can be written automatically for direct use in a combustion code.

To assess the validity of the method, the values for the steady state parameter Q given by Eq. (21) were computed using the 195 species iso-octane mechanism obtained after the elimination stage, for all cases and targets used in the validation of this mechanism. Additionally, the actual error in ignition delay time obtained when setting species in steady state one after the other was computed for each configuration. This error is correlated with the corresponding value of Q for the species. Results are presented in Fig. 13. A very small error of the order of 10^{-5} is introduced systematically that is due to numerics and grid resolution. A clear trend is observed, with species having small Q values introducing comparatively smaller error than species with large Q values. For example, a cut-off value of $Q = 10^{-12.25}$ identifies correctly 80 out of 83, that is, 96 % of the species introducing less than 0.2 % error on ignition delay time when set in steady state.

The evaluation of the coupled set of algebraic equations corresponds to the inversion of a matrix-vector system. To optimize the computational time required to perform this inversion, a search algorithm first identifies groups of inter-dependent species and re-orders the QSS species such that the resulting matrix is a block-triangular, easily invertible, matrix.

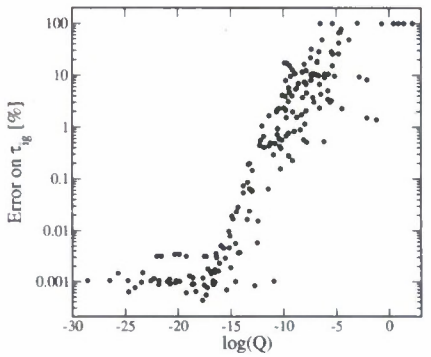

Figure 13: Maximum error in ignition delay time against the steady state parameter Q of each species when set in steady state over the specified range of initial conditions used for the reduction of the iso-octane mechanism.

2.2.4 Integration into a Multi-Stage Reduction Strategy

To exploit the reduction potential of the techniques presented above fully, the three reduction methods are combined through a multi-stage approach and applied to reduce the LLNL comprehensive iso-octane oxidation mechanism of Curran *et al.* [21]. The sample state space includes auto-ignition, plug-flow reactors, and premixed flames. The order of the reduction techniques is as follows. First, DRGEP removes negligible species and reactions until some error tolerance of about 15% for the chosen targets is reached. Removing more species at this stage would bring the error up considerably, as parts of some important parallel pathways would be removed. Although each channel individually does not contribute much to the global fluxes, discarding too many of them ends up introducing significant error. These pathways are lumped together in the next stage of reduction using the isomer lumping method presented above. Then, an additional stage of DRGEP can be applied to reduce the number of species further. Finally, QSSA are introduced to speed up the computational process. A final reduced mechanism is obtained, which consists of 57 species, 52 steady-state species, and 504 reactions. Comparisons of the results at various stages of reduction are shown in Figs. 14. Overall, the reduced mechanism reproduces correctly the detailed results for ignition timing, very lean oxidation in PFR, and flame propagation. The errors introduced by the reduction are small considering the high reduction ratio and everywhere negligible compared to the discrepancies with experimental data.

To appraise the benefits of the mechanism reduction, average computational costs are recorded for each skeletal or reduced mechanism and compared to the cost of using the full detailed model. Results are shown in Table 3 for homogeneous cases. The observed computational gain scales roughly like the square of the number of variables kept in the system, with a small additional benefit linked to the elimination of non-important reactions. A detailed flux analysis on detailed and reduced schemes shows that the various fuel consumption paths and their relative importance are retained for both low and high temperature oxidation [20].

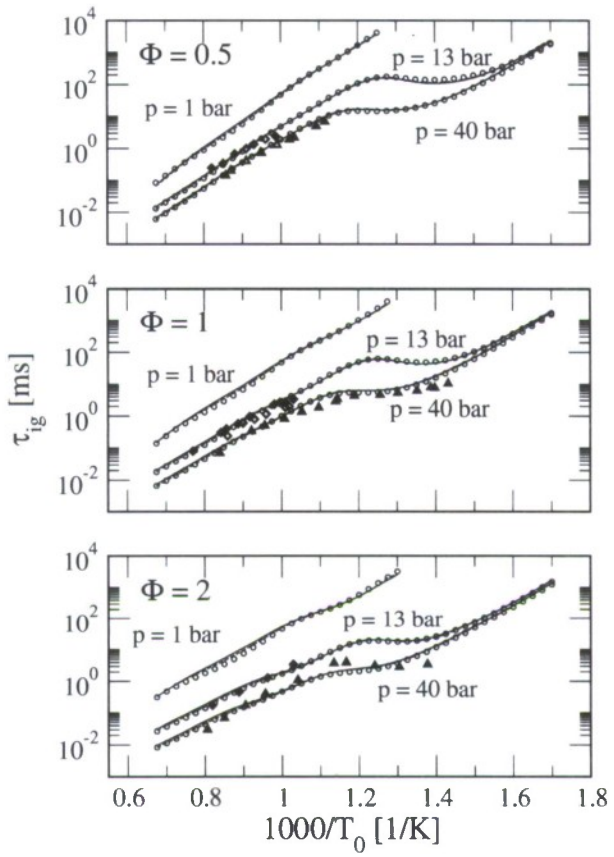

Figure 14: Ignition delay times for iso-octane. Comparison between experiments [25, 26, 27] (filled symbols), detailed (solid lines), 195 species skeletal (dashed lines), and 57 species reduced (open circles) mechanisms. Maximum error in ignition delay time is 34.94 %, average error is 10.86 %. Errors in the final concentration of the major products H_2O and CO_2 do not exceed 0.5 %.

	Number of species kept		Relative cost
Full mechanism	850	100 %	100
DRGEP (species elimination)	196	23.06 %	4.37
DRGEP (reaction elimination)	195	22.94 %	2.82
Lumping	134	15.76 %	2.16
DRGEP (extra)	109	12.82 %	1.65
QSS	57	6.70 %	0.98

Table 3: Relative computational cost for homogeneous simulations of the intermediate skeletal and final reduced mechanisms produced during the integrated multi-stage reduction of a detailed mechanism for iso-octane.

2.3 A Modular Approach to Model Transportation Fuel Chemistry

2.3.1 Selection of Surrogate Components and Composition

When designing a surrogate fuel, the goal is to identify a limited number of hydrocarbon molecules that can be blended into useful experimental fuels and modeled computationally [28]. Numerical considerations imply that kinetic, thermodynamic, and physical data of adequate quality are available for each of the molecules included in the set. Then, careful analysis of the type of application for which the surrogate is needed must be done, as the application will determine the set of relevant targets the surrogate will have to match. Potential targets are the heating value or energy content of the fuel, physical properties of the liquid fuel, boiling characteristics, reactivity, pollutant emissions, and class composition. A discussion of the applicability of each of these targets and how they can be evaluated for a fuel mixture can be found in [20].

Appropriate hydrocarbon candidates to be included in surrogate fuels should have been studied both experimentally and kinetically, so that validated models of sufficient accuracy are available. A review of available detailed chemical kinetic models for the oxidation of hydrocarbon molecules has been done by Simmie [29]. A certain number of such molecules and their potential relevance to the three major transportation fuels have been identified [28, 30, 31]. Following these guidelines, we have used in this work *n*-heptane, decane, and *n*-dodecane for the linear paraffin group, iso-octane and methyl-cyclohexane as branched paraffins, and benzene and toluene as aromatics.

A constrained optimization algorithm has been developed to facilitate the formulation of surrogate composition. The procedure relies on the fact that most properties described above are bulk properties and thus easily expressed as combinations of the properties of the individual components. For properties such as threshold sooting indices, for which data may not be available for all components, a group contribution approach has been adopted that estimates the properties of the mixture as function of the structural groups of the molecules included in the mixture. The procedure follows that described by Yan et al. [32], based on the initial work of Benson et al. [33]. Given a set of potential components, the algorithm returns the optimal composition that matches best the user-specified set of constraints.

2.3.2 Component Library Approach

Developing a chemical mechanisms for a transportation fuel surrogate will not be done only once but will be, rather, a dynamic process. CFD simulations require mechanisms that are as small as possible. This requirement definitely sets aside the "one surrogate fits all" approach and favors surrogates tightly tailored to the considered application, but even then, the composition provided by the optimization approach that relies on global characteristics may not be fully adequate for the problem at hand, and further experimental data may suggest some different composition or additional components. For example, the surrogate proposed by the jet fuel surrogate working group [31], composed of 50% *n*-decane, 25% *n*-butylbenzene, and 25% *n*-butylcyclohexane, was tested in a pressurized flow reactor and in a single cylinder research engine, and its characteristics in terms of flame ignition

and extinction in counterflow flames were compared to an average jet fuel. Although the surrogate matched the hydrogen-to-carbon ratio, it was consistently much more reactive than the fully-blended fuel, and therefore, was not an acceptable surrogate.

On the other hand, detailed chemical mechanisms undergo constant modifications, as the knowledge and understanding of the underlying kinetic processes increase, and these modifications must be incorporated into the reduced schemes for surrogate fuels as well. An additional challenge lies in the sizes of detailed mechanisms. If the detailed kinetic description of a single component involves up to a thousand species and several thousands reactions, combining several of these to form the model for a surrogate is clearly not a trivial task, and the chance of introducing incoherencies, such as truncated paths or involuntarily duplicated reaction pathways, is very high. Moreover, mechanisms of this size are impractical to use even in the simplest configurations. Numerical problems may arise, and, most importantly, no accurate and detailed analysis and validation of the mechanism can be carried out. Any reduction algorithm is then rendered inefficient or, at best, extremely slow.

We propose here a methodology to construct reduced kinetic models for surrogate fuels that is based on two principles:

- **Simplification:** Each type of mechanism manipulation has to be done at its simplest level. For example, reduction should be done on single component mechanisms, as it reduces both the size of the initial scheme and the extent of the validation domain. Also, combining kinetic data of single components to form mechanisms that can handle mixtures should be done with the smallest possible starting mechanisms, ideally skeletal ones.

- **Flexibility:** The addition of another component in the definition of the surrogate mixture should not require the entire process to be repeated. Instead, only the parts relevant to this extra molecule should be added. In the same way, if some additional feature, such as the ability to predict nitrogen oxides, is desired, it should be possible to add it without changing the core of the remaining mechanism.

The layout of the approach followed in this work is provided in Fig. 15. This modular approach relies on a library of skeletal mechanisms, or component library, to build kinetic schemes for mixtures efficiently. Given the type of fuel and the application, a surrogate composition can be devised through the optimization process presented above. On the chemistry side, existing detailed mechanisms for individual components are validated against experimental data, then reduced for various conditions to the skeletal level using two reduction techniques: the DRGEP method, and a chemical lumping technique. The collection of skeletal mechanisms forms the so-called component library, to which several specific modules can be added, such as a description of soot formation or NO_x chemistry. The surrogate composition and its future use dictate the choice of modules that have to be included in the combined skeletal mechanism, so that only the necessary kinetics are taken into account. Then, a second stage of reduction is applied that includes, for example, the introduction of quasi-steady state assumptions. The obtained reduced model can be

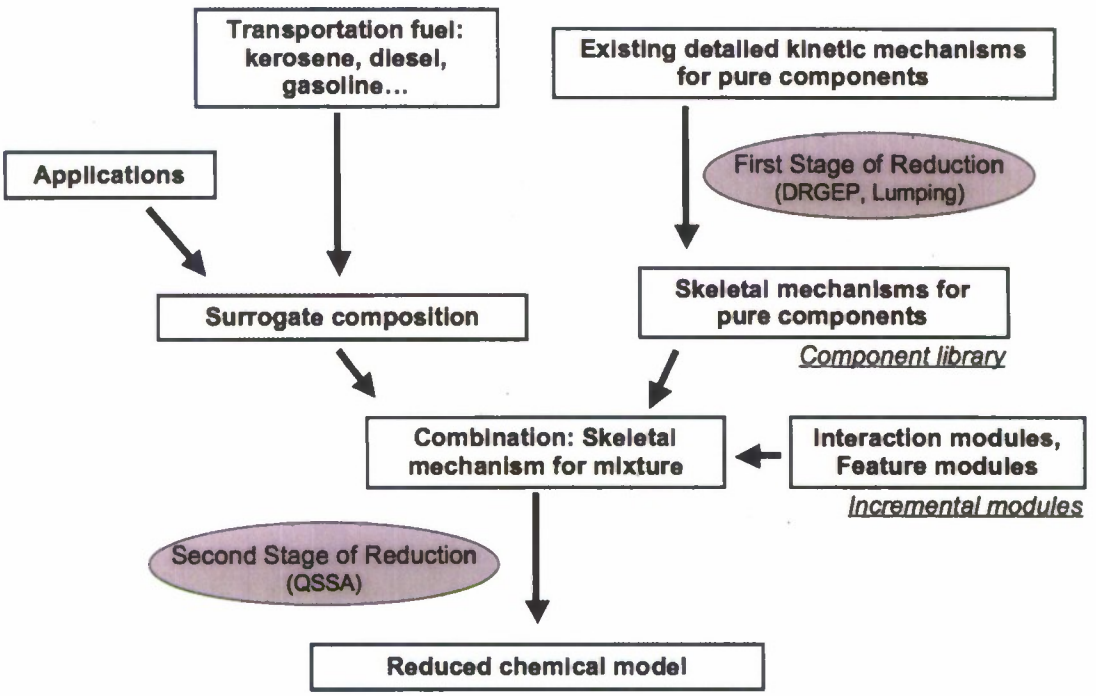

Figure 15: Layout and features of the component library approach.

validated using available experimental data. The results of this last step will provide additional constraints that have to be included in the surrogate definition phase, and the whole process can be repeated until an optimal surrogate is obtained. The major reduction steps, that is DRGEP and lumping, are done only once, which minimizes the turn-over time to produce the surrogate mechanism.

2.3.3 Assumptions and Challenges

The component library approach, and the efficiency of this approach, are based on two major assumptions. The first one is that two different large hydrocarbon molecules will interact during combustion only at the level of small radicals and decomposition products that are present already in both detailed mechanisms. Cross-reactions between fuel-specific molecules are neglected. The main argument to justify this assumption involves steric factors: unless the pressure is very high, the reactive sites of large molecules or radicals are much less accessible by another large species than a small radical such as OH. The validity of this assumption was shown experimentally by Klotz *et al.* [34] and numerically by Zhao *et al.* [35] for toluene/alkane mixtures. In case the cross-reactions between two compounds are shown to be important, incremental sets containing the relevant reactions could be added

in the library.

The second assumption is that not all reaction pathways are important for all configurations. This assumption allows the creation of modules through the reduction of the detailed mechanisms on complementary sub-domains of the parameter space. Then smaller multi-component mixtures are obtained by combining only the modules relevant to the application. The best example of this segregated approach is the temperature dependance of the hydrocarbon oxidation chemistry. The chemistry can be separated into a high temperature base chemistry and a low temperature module that can be superimposed on this base chemistry to represent the characteristic low temperature phenomena.

The chemistry reduction methods and how to determine an initial surrogate mixture composition have been described earlier. How the various modules from the component library and incremental sets may be assembled together to form a multi-component mechanism remains to be detailed. This step is simplified considerably by the fact that the detailed mechanisms have been reduced already to a skeletal level; however, even with this simplification, combining kinetic data from potentially very different sources is a non-trivial task. Species, thermodynamic and transport data, and elementary reactions need to be merged. To do this step most efficiently, an interactive set-up has been designed that automatically identifies identical species and reactions from the modules and records every multiple choice and incompatibility among the kinetic data sets. For example, species that have the same formula but different names would be identified. These species could be identical molecules, different isomers of the same species, or identical reactions with significantly different rate coefficients. These discrepancies cannot be resolved automatically; therefore, they are subjected to the user's expertise, who decides which option is the best available.

The component library approach described above has been used in several applications. For example, the modular approach is illustrated in [36] for the development of reduced models for a gasoline surrogate. In this study, specific modules for low-temperature ignition are identified and added to a reduced model describing premixed gasoline flames. Blanquart et al. [37] developed a kinetic mechanism describing PAH and soot formation, to which reduced modules for heptane and iso-octane oxidation were added automatically. A reduced module for soot formation was obtained using the methods described above and used to perform direct numerical simulations of soot formation in isotropic turbulence [38]. The next section illustrates in detail the development of a reduced model for a jet fuel surrogate.

2.3.4 Application to the development of chemical model for JP-8

As an application of the component library approach, the development of a skeletal model for a jet fuel surrogate was chosen. Conventional jet fuels, called Jet-A for civil applications and JP-8 for military, have a relatively high average carbon number, and corresponding representative hydrocarbons are difficult to handle experimentally. As a consequence, little experimental data currently exist to assist in the development of detailed chemical mechanisms for large hydrocarbons. As new data become available, the kinetic models will be validated and refined over a wider range of conditions; therefore, the present work does not

attempt to produce a surrogate model that will match perfectly the few data available for jet fuel. Instead, the focus is placed on the method used to generate the reduced model, especially the successive validation steps. If rigorous validation is performed, discrepancies in the results can be attributed mostly to inaccuracies in the detailed mechanisms and inadequacy of the initial choice of components, which is currently very limited. The subsequent development of better surrogate models will follow from improved initial experimental and kinetic data.

Surrogate Formulation The choice of the individual components for each hydrocarbon class was motivated mostly by the availability of a reasonably validated detailed chemical mechanism. They include *n*-heptane, iso-octane, and *n*-dodecane as alkanes, methylcyclohexane as naphthene, and benzene and toluene as aromatic molecules. The base mechanism is taken from Blanquart et al. [37]. This mechanism was developed specifically to represent soot formation and was validated extensively using experimental data for soot precursors, PAHs, and soot volume fractions. Mechanisms for *n*-heptane, iso-octane, and methyl-cyclohexane are taken from Lawrence Livermore National Laboratories [39, 21, 40], and *n*-dodecane is modeled by a semi-detailed mechanism developed by Wang et al. [41].

Three surrogate compositions were considered. The first one is neat *n*-dodecane. The second surrogate was developed by Violi et al. [42, 43] based on a number of criteria, including sooting tendency and distillation characteristics. The third one is obtained through the optimization procedure described previously, by prescribing the hydrogen-to-carbon ratio, the average carbon number, the average composition in terms of hydrocarbon classes, the cetane number, and the sooting tendency of the fuel. Only three different components were included in the optimization, namely *n*-dodecane, methyl-cyclohexane, and toluene. The resulting composition and a comparison of the properties of the three surrogates are shown in table 4.

		Average Jet Fuel	Neat Dodecane	Surrog. 1	Surrog. 2
Composition [% mol]	Dodecane	N/A	100	73.5	45
	Iso-octane		0	5.5	0
	MCH		0	10	26.1
	Toluene		0	10	28.9
	Benzene		0	1	0
H/C ratio		1.91	2.17	2.09	1.09
Formula		$C_{11}H_{21}$	$C_{12}H_{26}$	$C_{10.7}H_{22.3}$	$C_{9.3}H_{17.7}$
Hydrocarbon composition [% vol]	Paraffins	~60	100	88	62
	Naphthenes	~20	0	6.4	20
	Aromatics	~18	0	5.6	18
Cetane number		~42.7	80	73.4	58
Threshold sooting index		~15	5.2	9.3	16.3

Table 4: Compositions for jet fuel surrogate used in comparison with experimental measurements.

The domain of applicability of the reduced surrogate models was chosen to represent the most probable operation conditions found in gas-turbine engines, namely high temperature, atmospheric to high pressures, and lean-to-rich conditions. Auto-ignition and premixed conditions are included in the reduction procedure, as newly designed engines tend to run partially premixed, which inevitably leads to the necessity to control auto-ignition at operating conditions [31]. The detailed mechanisms for the individual components are reduced independently to a skeletal level using DRGEP and chemical lumping. Then, the resulting modules are combined together, with the base mechanism of Blanquart et al. [37] retained as reference. The resulting scheme is a multi-component mechanism containing only 181 species, able to accurately describe the oxidation of *n*-heptane, iso-octane, *n*-dodecane, methyl-cyclohexane, benzene, toluene, and the soot precursor acetylene. Validation is performed at each stage, and includes:

- Comparison of the detailed mechanism with experimental data
- Comparison of simulations obtained using the single component skeletal mechanism and the detailed mechanism from which it is extracted
- Comparison of simulations obtained for each individual component using the combined skeletal mechanism and the corresponding single component detailed mechanism
- Assessment of the performance of the combined surrogate mechanism by comparing simulation results with experimental data for jet fuels.

Comparisons with experimental data are described in detail in [20]. The pure components mentioned above were extensively studied in a wide range of configurations, such as auto-ignition, plug-flow reactors, premixed and counter-flow flames for various temperatures, pressure and equivalence ratios. The multi-component model showed good agreement with both the original detailed schemes and the various experimental sets.

Simulation results for ignition delay times of jet fuel are shown in Fig. 16. Figure 16(a) compares two different pressures, 20 and 50 atm, Fig. 16(b) compares two levels of dilution for stoichiometric mixtures of jet fuel and air, and Fig. 16(c) compares ignition delay times for two different equivalence ratios, 0.5 and 1. The conclusions are similar in each of the cases. First, all surrogates over-predict auto-ignition by a factor two to three. New experimental data from Vasu et al. [44] show that *n*-dodecane/air mixtures ignition delay times are close to those of jet fuel. As *n*-dodecane is the major component in all surrogates, this observation tends to indicate that the *n*-dodecane mechanism does not predict auto-ignition well. Also, *n*-dodecane is the component that ignites the fastest. As surrogate #2 contains less of the large alkane than the others, this surrogate shows the biggest discrepancy compared to experiments at high temperature.

A second observation concerns the onset of the NTC region. Experimental data show no NTC behavior for temperatures larger than 850 K. However, both pure *n*-dodecane and Surrogate #1 have a strong NTC behavior for temperatures around 1000 K. This NTC is much weaker for Surrogate #2. Disregarding the shift due to the slow ignition of

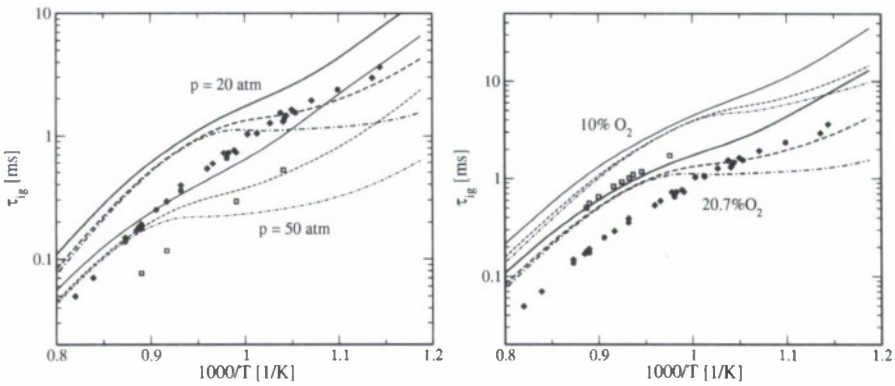

(a) Effect of pressure ($\phi = 1, 20.7\%\,O_2$).

(b) Effect of X_{O_2} ($\phi = 1$, 20 atm).

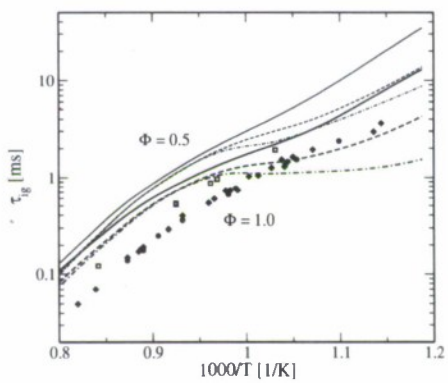

(c) Effect of equivalence ratio (20.7% O_2, 20 atm).

Figure 16: Auto-ignition of JetA/JP-8. Comparison between experimental data (squares, [44]), and simulation results obtained with pure dodecane (dash-dotted lines), surrogate #1 (dashed lines) and surrogate #2 (solid lines).

n-dodecane in the simulation, Surrogate #2 better represents the jet fuel experimental data.

Experimental and simulated species concentration profiles obtained in a premixed atmospheric kerosene flame, with an initial temperature of 473 K [45], are shown in Fig. 17. Prediction of oxygen consumption and major product formation, such as CO and CO_2, is in acceptable agreement with the measurements. The precise compositions of the surrogates have very little effect on the evolution of the major species; however, the concentration of specific intermediate species clearly are impacted by the initial composition. For example, neat *n*-dodecane tends to produce very little benzene, whereas the presence of toluene and benzene from the inlet increases drastically the maximum concentration of benzene in the flame. Other common intermediates that are natural decomposition products of any sufficiently large hydrocarbon fuel are produced in similar quantity by the three surrogates.

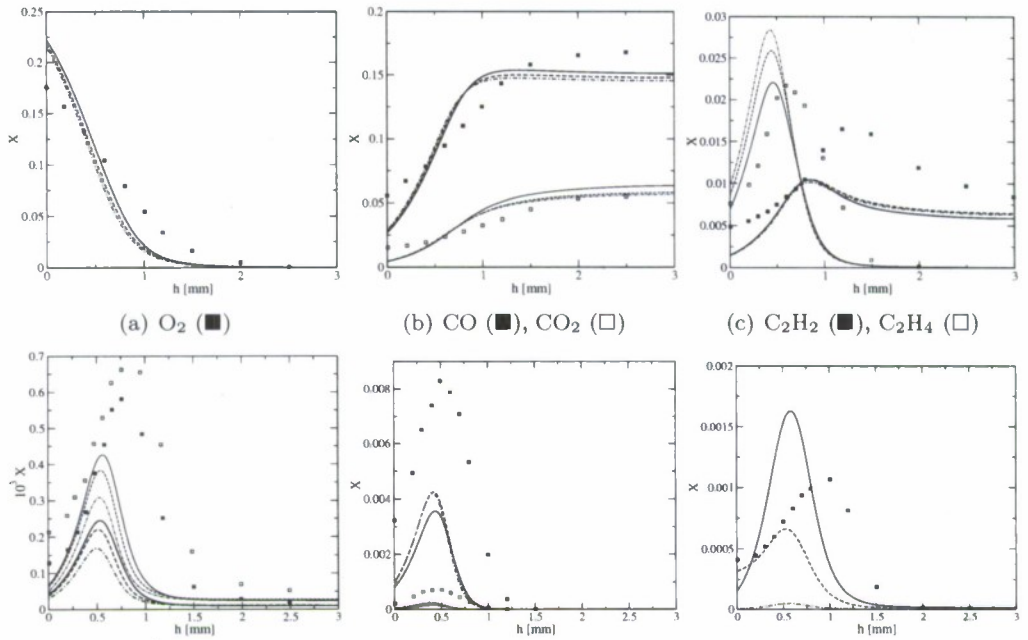

(a) O_2 (■) (b) CO (■), CO_2 (□) (c) C_2H_2 (■), C_2H_4 (□)

(d) Allene (■), Propyne (□) (e) C_3H_6 (■), C_3H_8 (□) (f) Benzene (■)

Figure 17: Premixed burner-stabilized kerosene flame. Comparison between experimental data (squares, [45]), and simulation results obtained with pure dodecane (dash-dotted lines), surrogate #1 (dashed lines) and surrogate #2 (solid lines).

The present experimental validation set is not sufficient to conclude with certitude on the performances of the tested surrogates except, perhaps, for the neat *n*-dodecane case that is clearly not representative of either jet fuel auto-ignition or flame oxidation. Indeed, too much uncertainty still exists in the detailed kinetic models considered in this study; however, should any of these mechanisms be improved in the near future, only a few steps need to be repeated, namely the reduction of this particular mechanism, combination with the other skeletal schemes, and validation steps for all components. Provided that the reference mechanism is left unchanged, this latter stage should not introduce any problems in the untouched components, and the whole process is expected to be quite fast.

3 Conclusions

In this project, we have focussed on two topics: advanced combustion models for large-eddy simulations (LES) and reduced chemical mechanisms for JP-8 surrogate fuels. We have made substantial progress on both of these topics. The aim of the combustion LES modeling part was to advance the models for non-premixed and premixed combustion towards a generalized combustion model that covers all combustion regimes. Towards this end, we have made three major model advancements. First, a dynamic model for the turbulent burning velocity was developed. This model eliminates the use of model constants in the G-equation formalism, which is used to compute the flame position. The propagation term appearing in this equation now is computed dynamically. The model formulation comes from applying the constraint that the model must produce consistently the same flame behavior at all LES filter levels. Additionally, a new filtering approach has been developed that now allows for the use of the volumetric filters. This approach enables explicit filtering of the flame on the LES test filter length scale. Direct numerical simulations (DNS) of flame propagation in a turbulent flow were performed to assess the model. The model was found to predict the DNS results very accurately. Advantages of the new model were found specifically in the early development of the turbulent flame before a statistical steady state is reached.

Second, a flame structure model was developed. This additional model is necessary because the solution of the G-equation provides only the mean position of a given temperature iso-surface, typically chosen to be that of the inner layer temperature. For a sub-filter Damköhler number larger than unity, the entire flame appears on the sub-filter scale and requires no further treatment; however, for small Damköhler numbers, the flame is resolved only partially and cannot be described by the G-equation alone. In the flame structure model, an equation for the reaction progress variable is solved in addition to the G-equation. This equation shows a sharp jump across the filtered flame and therefore cannot be used to track the flame accurately. In the new formulation, both the transport term and the chemical source term are modeled such that the filtered position of the inner layer predicted from the progress variable equation is consistent with that of the G-equation. This treatment ensures the correct propagation speed, and the filtered temperature and density then can be computed from the progress variable field. Our models for non-premixed combustion also use a reaction progress variable equation. The progress variable therefore provides a way to merge the two models for premixed and non-premixed combustion. The source terms, however, must be modeled as a function of the combustion regime.

Third, a formalism to detect the combustion regime locally was developed. The so-called flame index was proposed previously, but we have shown that this quantity is too simplistic and does not work in general. Our method is based on an asymptotic analysis of the limiting cases. The existence of the flame structure model and a combustion regime identifier provide a basis for developing a consistent generalized model that works across different combustion regimes.

In the chemistry part of the project, we have focussed on two issues, the component li-

brary approach and the automatic reduction procedure. In the component library approach, reduced chemical mechanisms are stored as modules in a component library. Several modules could be included in the component library for each fuel component, such as a basis module for high-temperature chemistry and additional incremental sets for low-temperature chemistry and soot precursors. In addition to populating the component library with several components, we have made the reduction process more automatic and have developed tools for the automatic combination of mechanisms comprised of different components. The automatic reduction procedure itself was developed by refining the DRGEP method. This method now is used to eliminate species and reactions. Additionally, we have introduced an automatic procedure to select steady state species, and we have developed a new accurate method for species lumping. The resulting automatic reduction procedure is based on the combination of all these approaches. The method was tested on the largest available mechanisms for various hydrocarbon molecules, such as *n*-heptane, iso-octane, and methylcyclohexane. The mechanisms were reduced automatically, and the component library approach was validated successfully. The resulting mechanism is quite small compared to the original, but similarly small mechanisms have been achieved using other reduction methods. What is unique about our approach is that, in contrast to other methods, the entire reduction procedure is automatic and based on a single evaluation of the production rates with the detailed mechanism. The reduction, therefore, is cheap and occurs all at once. This feature is important, since it could form the basis of an automatic adaptive chemistry approach, where the reduction is performed automatically during a reactive computational fluid dynamics simulation.

4 Participating Personnel

During the reporting period, the PI and two graduate students, Perrine Pepiot and Edward W. Knudsen, have been supported within the present research grant.

5 List of Submitted and Accepted Publications in Reporting Period

1. Moureau, V., Fiorina, B., Pitsch, H. A level set formulation for premixed combustion LES considering the turbulent flame structure, Combust. Flame, in press, 2008.

2. Blanquart, G., Pepiot-Desjardins, P., Pitsch, H. Chemical Mechanism for High Temperature Combustion of Engine Relevant Fuels with Emphasis on Soot Precursors, Comb. Flame, 156 (3), 588-607, 2009.

3. Knudsen, E., Pitsch, H., A general flamelet transformation useful for distinguishing between premixed and non-premixed modes of combustion, Comb. Flame, 156 (3), 678-696, 2009.

4. Jerzembeck, S., Peters, N., Pepiot-Desjardins, P., Pitsch, H., Laminar Burning Velocities at High Pressure for Primary Reference Fuels and Gasoline: Experimental and Numerical Investigation, Comb. Flame, 156 (2), 292-301, 2009.

5. Pepiot-Desjardins, P., Pitsch, H., An automatic chemical lumping method for the reduction of large chemical kinetic mechanisms, Combust. Theory. Mod., 12 (6), pp. 1089-1108, 2008.

6. Knudsen, E., Pitsch, H., A Dynamic Model for the Turbulent Burning Velocity for LES of Premixed Combustion, Comb. Flame, 154 (4), pp. 740-760, 2008.

7. Pepiot-Desjardins, Pitsch, H., An efficient error propagation based reduction method for large chemical kinetic mechanisms, Comb. Flame, 154 (1-2), pp. 67-81, 2008.

6 Interactions and Transitions

During this project, we had several interactions with Dr. Roquemore and Dr. Zelina from AFRL, and on a more technical level with Dr. Sekar from AFRL. We have transitioned our unstructured multi-physics LES code to Dr. Sekar by installing the code on AFRL computers. He will use the code for reactive multi-phase combustor simulations. We have also provided Dr. Sekar with reduced chemical mechanisms. In addition, we had several interactions regarding combustion modeling with Rolls Royce, Pratt & Whitney, Honeywell, and more recently with GE.

7 Patents and Inventions

None

References

[1] E. Knudsen and H. Pitsch. A general flamelet transformation useful for distinguishing between premixed and non-premixed modes of combustion. *Combust. Flame*, 156(3):678–696, 2009.

[2] M. Ihme and H. Pitsch. Prediction of extinction and reignition in nonpremixed turbulent flames using a flamelet/progress variable model. 2. Application in LES of Sandia flames D and E. *Combust. Flame*, 155(1):90–107, 2008.

[3] M. Boileau, G. Staffelbach, B. Cuenot, T. Poinsot, and C. Berat. LES of an ignition sequence in a gas turbine. *Combust. Flame*, 154(1-2):2–22, 2008.

[4] K.-J. Nogenmyr, C. Fureby, X. S. Bai, P. Petersson, R. Collin, and M. Linne. Large Eddy simulation and laser diagnostic studies on a low swirl stratified premixed flame. *Combust. Flame*, 155(3):357–368, 2008.

[5] E. Knudsen and H. Pitsch. A dynamic model for the turbulent burning velocity for large eddy simulation of premixed combustion. *Combust. Flame*, 154(4):740–760, 2008.

[6] H. Pitsch and L. Duchamp De Lageneste. Large-eddy simulation of premixed turbulent combustion using a level set approach. *Proc. Comb. Inst.*, 29:2001–2008, 2002.

[7] P. Domingo, L. Vervisch, and J. Réveillon. DNS analysis of partially premixed combustion in spray and gaseous turbulent flame-bases stabilized in hot air. *Combust. Flame*, 140:172–195, 2005.

[8] N. Peters. *Turbulent Combustion*. Cambridge Univ. Press, Cambridge, UK, 2000.

[9] O. Colin, F. Ducros, D. Veynante, and T. Poinsot. A thickened flame model for large eddy simulations of turbulent premixed combustion. *Phys. Fluids*, 12(7):1843–1862, 2000.

[10] R. Knikker, D. Veynante, and C. Meneveau. A dynamic flame surface density model for large eddy simulation of turbulent premixed combustion. *Phys. Fluids*, 16(11):L91–L94, 2004.

[11] V. Moureau, B. Fiorina, and H. Pitsch. A level set formulation for premixed combustion LES considering the turbulent flame structure. *Combust. Flame*, 156(4):801–812, 2009.

[12] H. Yamashita, M. Shimada, and T. Takeno. A numerical study on flame stability at the transition point of jet diffusion flames. *Proc. Comb. Inst.*, 26:27–34, 1996.

[13] V. Favier and L. Vervisch. Edge flames and partially premixed combustion in diffusion flame quenching. *Combust. Flame*, 125:788–803, 2001.

[14] B. Fiorina, O. Gicquel, L. Vervisch, S. Carpentier, and N. Darabiha. Approximating the chemical structure of partially premixed and diffusion counterflow flames using FPI flamelet tabulation. *Combust. Flame*, 140:147–160, 2005.

[15] B. Bédat and R. K. Cheng. Experimental study of premixed flames in intense isotropic turbulence. *Combust. Flame*, 100:485–494, 1995.

[16] R. K. Cheng. Velocity and scalar characteristics of premixed turbulent flames stabilized by weak swirl. *Combust. Flame*, 101:1–14, 1995.

[17] P. Petersson, J. Olofsson, C. Brackman, H. Seyfried, J. Zetterberg, M. Richter, M. Aldén, M. A. Linne, R. K. Cheng, A. Nauert, D. Geyer, and A. Dreizler. Simultaneous PIV/OH-PLIF, rayleigh thermometry/OH-PLIF and stereo PIV measurements in a low-swirl flame. *Applied Optics*, 46(19):3928–3936, 2007.

[18] P. Pepiot-Desjardins and H. Pitsch. An Efficient Error Propagation Based Reduction Method for Large Chemical Kinetic Mechanisms. *Combust. Flame*, 154:67–81, 2008.

[19] P. Pepiot-Desjardins and H. Pitsch. An Automatic Chemical Lumping Method for the Reduction of Large Chemical Kinetic Mechanisms. *Combust. Th. Model.*, 12:1089–1108, 2008.

[20] P. Pepiot. *Automatic strategies to model transportation fuel surrogates.* PhD thesis, Stanford University, 2008.

[21] H. J. Curran, P. Gaffuri, W. J. Pitz, and C. K. Westbrook. A comprehensive modeling study of iso-octane oxidation. *Combust. Flame*, 129:253–280, 2002.

[22] C. M. Bishop. *Neural Networks for Pattern Recognition.* Oxford University Press, Oxford, 1995.

[23] P. Pepiot and H. Pitsch. Systematic Reduction of Large Chemical Kinetic Mechanisms. *Proceedings of the 4th Joint Meeting of the U.S. Sections of the Combustion Institute*, 2005.

[24] S. S. Ahmed, F. Mauss, G. Moréac, and T. Zeuch. A Comprehensive and Compact *n*-Heptane Oxidation Model Derived Using Chemical Lumping. *Phys. Chem. Chem. Phys.*, 9:1107–1126, 2007.

[25] D.F. Davidson, B.M. Gauthier, and R.K. Hanson. Shock Tube Ignition Measurements of Iso-Octane/Air and Toluene/Air at High Pressures. *Proc. Combust. Inst.*, 30:1175–1182, 2005.

[26] K. Fieweger, R. Blumenthal, and G. Adomeit. Self-Ignition of S.I. Engine Model Fuels: a Shock Tube Investigation at High Pressure. *Combust. Flame*, 109:599–619, 1997.

[27] C. V. Callahan, T. J. Held, F. L. Dryer, R. Minetti, M. Ribaucour, L. R. Sochet, T. Faravelli, P. Gaffuri, and E. Ranzi. Experimental Data and Kinetic Modeling of Primary Reference Fuel Mixtures. *Proc. Combust. Inst.*, 26:739–746, 1996.

[28] W. J. Pitz, N. P. Cernansky, F. L. Dryer, F. N. Egolfopoulos, J. T. Farrell, D. G. Friend, and H. Pitsch. Development of an Experimental Database and Chemical Kinetic Models for Surrogate Gasoline Fuels, SAE 2007-01-0175, 2007.

[29] J. M. Simmie. Detailed Chemical Kinetic Models for the Combustion of Hydrocarbon Fuels. *Prog. Energy Combust. Sci.*, 29:599–634, 2003.

[30] J. T. Farrell, N. P. Cernansky, F. L. Dryer, D. G. Friend, C. A. Hergart, C. K. Law, R. M. McDavid, C. J. Mueller, A.K. Patel, and H. Pitsch. Development of an Experimental Database and Kinetic Models for Surrogate Diesel Fuels, SAE 2007-01-0201, 2007.

[31] M. Colket, T. Edwards, S. Williams, N.P. Cernansky, D.L. Miller, F. Egolfopoulos, P. Lindstedt, K. Seshadri, F.L. Dryer, C.K. Law, D. Friend, D.B. Lenhert, H. Pitsch, A.F. Sarofim, M. Smooke, and W. Tsang. Development of an Experimental Database and Kinetic Models for Surrogate Jet Fuels, AIAA 2007-770, 2007.

[32] S. Yan, E. G. Eddings, A. B. Palotas, R. J. Pugmire, and A. F. Sarofim. Prediction of Sooting Tendency for Hydrocarbon Liquids in Diffusion Flames. *Energy and Fuels*, 19:2408–2415, 2005.

[33] S. W. Benson. *Thermochemical Kinetics : Methods for the Estimation of Thermochemical Data and Rate Parameters.* Wiley, New York, 1976.

[34] S. D. Klotz, K. Brezinsky, and I. Glassman. Modeling the Combustion of Toluene-Butane Blends. *Proc. Combust. Inst.*, 27:337–344, 1998.

[35] Z. Zhao, M. Chaos, A. Kazakov, P. Golkulakrishnan, M. Angioletti, and F. Dryer. Fuel Chemistry Models for Simulating Gasoline Kinetics in Internal Combustion Engines, 31st International Symposium on Combustion, Work in progress Poster No. 2C-27, Heidelberg, Germany, 2006.

[36] S. Jerzembeck, N. Peters, P. Pepiot-Desjardins, and H. Pitsch. Laminar Burning Velocities at High Pressure for Primary Reference Fuels and Gasoline: Experimental and Numerical Investigation. *Combust. Flame*, 156:292–301, 2008.

[37] G. Blanquart, P. Pepiot-Desjardins, and H. Pitsch. Chemical Mechanism for High Temperature Combustion of Engine Relevant Fuels with Emphasis on Soot Precursors. *Combust. Flame*, 2008, submitted.

[38] F. Bisetti, G. Blanquart, M. E. Mueller, P. Pepiot-Desjardins, and H. Pitsch. Direct numerical simulation of soot formation in turbulent nonpremixed ames with nite rate

chemistry and detailed soot dynamics. *2009 Joint Meeting of the U.S. Section of the Combustion Institute, University of Michigan, Ann Arbor, MI, May 17-20*, 2009.

[39] H. J. Curran, P. Gaffuri, W. J. Pitz, and C. K. Westbrook. A comprehensive modeling study of n-heptane oxidation. *Comb. Flame*, 114:149–177, 1998.

[40] W. J. Pitz, C. V. Naik, T. Ni Mhaolduinc, C. K. Westbrook, H. J. Curran, J. P. Orme, and J. M. Simmie. Modeling and Experimental Investigation of Methylcyclohexane Ignition in a Rapid Compression Machine. *Proc. Combust. Inst.*, 31:267–275, 2007.

[41] H. Wang X.Q. You, F.N. Egolfopoulos. Detailed and Simplified Kinetic Models of n-Dodecane Oxidation : The role of Fuel Cracking in Aliphatic Hydrocarbon Combustion. *Proc. Combust. Inst.*, 32, 2008, submitted.

[42] A. Violi, S. Yan, E. G. Eddings, A. F. Sarofim, S. Granata, T. Faravelli, and E. Ranzi. Experimental formulation and kinetic model for jp-8 surrogate mixtures. *Comb. Sci. Tech.*, 174:399–417, 2002.

[43] E.G. Eddings, S. Yan, W. Ciro, and A.F. Sarofim. Formulation of a Surrogate for the Simulation of Jet Fuel Pool Fires. *Combust. Sci. Tech.*, 177:715–739, 2005.

[44] S. S. Vasu, D. F. Davidson, and R. K. Hanson. Jet fuel Ignition Delay Times: Shock Tube Experiments over Wide Conditions and Surrogate Model Predictions. *Combust. Flame*, 152:125–143, 2008.

[45] C. Doute, J. L. Delfau, R. Akrich, and C. Vovelle. Chemical Structure of Atmospheric Pressure Premixed n-Decane and Kerosene Flames. *Combust. Sci. Tech.*, 106:327–344, 1995.